Advanced Biomaterials for Regenerative Dentistry in Oral Health Care – Original Research Article

JABFM Journal of Applied Biomaterials & Functional Materials

Journal of Applied Biomaterials & Functional Materials
1–12

DOI: 10.1177/22808000241296663
journals.sagepub.com/home/jbf
Sage

The microstructure, composition, physical properties, and bioactivity of calcium silicate cement prototypes for vital pulp therapies

Marina Vega-González[1], Rubén Abraham Domínguez-Pérez[2,3], Ana Edith Higareda-Mendoza[4], Ricardo Domínguez-Pérez[2], León Francisco Espinosa-Cristóbal[5] and Roberto Gustavo Sánchez-Lara y Tajonar[3]

Abstract

Hydraulic calcium silicate cements (HCSCs) are valuable for various dental procedures. However, several reports document inherent limitations and complaints about their high costs, hindering accessibility in low—and middle-income countries. This study aimed to characterize four low-cost HCSC prototypes to show their microstructure, composition, and fundamental physical properties. Four HCSC prototypes were formulated: 1- calcium silicate powder with 17.5 wt. % replacement of calcium tungstate, 2- calcium silicate powder with 17.5 wt. % replacement of zirconium oxide, 3- calcium silicate powder with 17.5 wt. % replacement of calcium tungstate and 2.5 wt. % of zirconium oxide and 4- calcium silicate powder with 10 wt. % replacement of calcium tungstate and 10 wt. % replacement of zirconium oxide. Scanning electron microscopy, energy-dispersive X-ray spectroscopy, and X-ray diffraction were used to assess their microstructure and composition. Additionally, radiopacity, setting time, solubility, pH, and in vitro bioactivity were evaluated at different time points and contrasted with controls (Mineral trioxide aggregate –MTA Angelus- and Intermediate restorative material -IRM-). Their production cost was significantly lower than commercially available HCSCs. All prototypes exhibited a microstructure and composition comparable to MTA Angelus. All the prototypes exhibited radiopacity exceeding 3 mm of aluminum and shorter initial and final setting times than MTA Angelus. The solubility of some prototypes closely adhered to the ISO standard recommendation of 3% after 1 day, and all promoted an alkaline pH and the formation of calcium/phosphate precipitates. These promising findings suggest the potential clinical application of these prototypes. However, further research is necessary to evaluate their mechanical and biological properties for definitive clinical use.

Keywords

Calcium silicate cements, radiopacity, setting time, solubility, pH, calcium phosphate nucleation

Date received: 15 July 2024; revised: 9 September 2024; accepted: 4 October 2024

[1]Institute of Geosciences, Universidad Nacional Autónoma de México, Santiago de Querétaro, Querétaro, México
[2]Laboratory of Multidisciplinary Dentistry Research, Facultad de Medicina, Universidad Autónoma de Querétaro, Santiago de Querétaro, Querétaro, México
[3]Endodontic Specialization Program, Facultad de Medicina, Universidad Autónoma de Querétaro, Santiago de Querétaro, México
[4]División de Estudios de Posgrado de la Facultad de Ciencias Médicas y Biológicas "Dr. Ignacio Chávez", Universidad Michoacana de San Nicolás de Hidalgo, Morelia, Michoacán, Mexico
[5]Master Program in Dental Sciences, Stomatology Department, Institute of Biomedical Sciences, Autonomous University of Juarez, Ciudad Juárez, México

Corresponding author:
Rubén Abraham Domínguez-Pérez, Laboratory of Multidisciplinary Dentistry Research, Facultad de Medicina, Universidad Autónoma de Querétaro, Clavel #200, Prados de La Capilla, Santiago de Querétaro, Qro 76176, México.
Email: dominguez.ra@uaq.mx

Table 1. Powder ratios of the HCSC prototypes and their assigned names.

Prototype name	Formulation
w175	CS-base with 17.5 wt. % replacement of m-$CaWO_4$
z175	CS-base with 17.5 wt. % replacement of m-ZrO_2
w175z25	CS-base with 17.5 wt. % replacement of m-$CaWO_4$ and 2.5 wt. % of m-ZrO_2
w10z10	CS-base with 10 wt. % replacement of m-$CaWO_4$ and 10 wt. % of m-ZrO_2

Introduction

Thirty years ago, hydraulic calcium silicate cements (HCSCs) revolutionized dentistry with the introduction of mineral trioxide aggregate (MTA).[1] This was due to its combination of appropriate physical, mechanical, and biological properties, but mainly because of their bioactivity, characteristic of these materials and considered the foundation for their favorable properties.[2]

HCSCs mainly comprise di- and tri-calcium silicate and possess the capability to set in humid and wet environments. They were primarily proposed for root-end filling,[3] perforation repair,[4] and apical barrier formation.[5] Later they were used in direct pulp capping,[6] or vital pulp therapies.[7] However, several reports have documented inherent limitations, mainly long setting time,[8] tooth discoloration,[9] and difficult manipulation,[10] in addition to complaints about their very high cost.[11] These issues spurred researchers worldwide to propose improvements.[12] Several more materials were developed throughout the years, mainly by modifying the original formula. The initial focus was to overcome the shortcomings and, later, to improve their general physical, mechanical, and biological properties, allowing for the development of a wide variety of products.[13] To this day, it is well known that even minor chemical differences[14,15] or the inclusion of different additives,[16–20] as well as differences in the size and shape of the particles, will largely determine the physical, mechanical, and biological properties that each HCSC will present under different conditions.[21] This will undoubtedly influence the clinical outcome of treatment.[22]

A significant body of knowledge now exists concerning HCSCs. Commercial entities actively leverage this knowledge to constantly develop novel materials with improved properties. While not yet reaching complete optimization, these materials approach a state of perfection by incorporating the minimum requisite characteristics to elicit a favorable tissue response, ultimately promoting successful treatment outcomes.[13] The only aspect that has not yet been solved is their high cost, which has been criticized since the first of these came on the market, but that could never really be resolved, even though their cost has continued to increase for the new ones as they are more complex materials (unidosis capsules, ready-to-use preparations, materials with diverse additives). This situation may be less significant in developed countries with accessible healthcare. However, it is a significant barrier in low- and middle-income countries. The high cost of HCSCs restricts access to treatments that can significantly impact patients' health and quality of life, as demonstrated in a recent pilot clinical trial where vital pulp therapies (VPT) were successfully performed on cases of irreversible pulpitis or deep caries, avoiding dental extractions.[7] Unfortunately, due to the high cost of these materials, this treatment cannot be routinely provided to the population in public primary care clinics.[7]

For this reason, the Multidisciplinary Dentistry Research Laboratory (Faculty of Medicine, Universidad Autónoma de Querétaro, Mexico) has undertaken a multi-year effort to design, produce, and evaluate several experimental HCSCs. These prototypes prioritize the optimization of physical, mechanical, and biological properties while minimizing production costs, aligning with sustainable development and environmental considerations.[23] To date, promising prototypes have undergone preliminary evaluation but require detailed ones currently being carried out. This study aimed to characterize four HCSC prototypes to show their microstructure and composition, as well as to evaluate their radiopacity, setting time, solubility, pH, and in vitro bioactivity, as these are the most critical physical properties of a material used in VPT. These properties were also compared with two commercial materials, MTA Angelus (Angelus, Londrina, Brazil) and a zinc-oxide eugenol-based material (IRM; Dentsply Sirona, Charlotte, NC, USA).

Methods

Four HCSC prototypes were formulated using the following materials: calcium-silicate powder (CPC-30R-B, Cemex, Mexico) subjected to a 60°C thermal treatment during 24 h (CS-base), calcium tungstate (Cat: 248665, Sigma Aldrich) ball-milled for 20 h (m-$CaWO_4$) and zirconium oxide (Cat.230693, Sigma Aldrich) ball-milled for 20 h (m-ZrO_2). The prototypes were prepared as presented in Table 1. All formulations were mixed in a grinding chamber for 12 h at 60°C to ensure complete integration of all constituents while preventing moisture absorption from the environment.

MTA Angelus and IRM were used as control materials. These controls were prepared according to their manufacturer's instructions,[24,25] while the HCSC prototypes were manually prepared with distilled water at a water-to-powder ratio of 0.35 to achieve a putty consistency.

Microstructure and composition of the HCSCs in powder and set forms

Each prototype and MTA Angelus (powder and set forms) were placed upon carbon tapes and imaged with a scanning electron microscope (SEM, Hitachi TM1000, Mito City, Japan) operating at 15 kV, with a backscattered detector and equipped with energy-dispersive X-ray spectroscopy (EDX; Oxford Instruments, Abingdon, UK). EDX data was used to identify the elements in each of the presentations. The analysis was performed in triplicate for each sample. In addition, crystalline phases were identified through X-ray diffraction (XRD). Powder forms of all HCSCs were analyzed using a Miniflex 600 equipment (Rigaku, Tokyo, Japan) with copper radiation Kα 1.5406 Å, generated at 30 kV and 30 mA, between 10 and 70 degrees 2θ, with a step of 0.02 degrees and a scan speed of 1° per minute. Phases were identified according to the ICDD database (International Centre for Diffraction Data, Newtown Square, PA, USA).

Radiopacity

The radiopacity of each HCSC prototype and controls was evaluated according to ISO 6876:2012 standard. Eight specimens were prepared using molds with a diameter of 7 ± 0.1 mm and a height of 1 ± 0.1 mm. The specimens were stored at 37°C and 95% relative humidity for 7 days to ensure complete setting.

Subsequently, specimens were radiographed alongside a 1 mm increment aluminum step wedge (1–10 mm thickness) positioned on a digital radiographic system (Acteon/MicroImagem, Indaiatuba, Brazil). Digital radiographs were acquired using a standard X-ray unit with an exposure time of 0.50 s, 10 mA current, 65 ± 5 kV tube voltage, and a source-to-image distance of 30 cm. The optical densities of the test materials were evaluated using the ImageJ software (v1.33, NIH, Bethesda, MD, USA), and the grey-scale values (density measurements) were converted into mm equivalents of aluminum.

Setting time

Setting times were determined according to the ASTM C266-08 standard.[26] Five silicon molds (diameter: 10.0 mm ± 0.1 mm, height: 2.0 mm ± 0.1 mm) were filled with each material. Following a 5-min incubation at 37°C and 99% relative humidity, the initial setting time was assessed using a Gilmore-type needle (diameter: 2.0 mm ± 0.1 mm, height: 5 mm, weight: 100 g ± 5 g). It was carefully lowered onto the specimen surface without additional pressure. This procedure was repeated every 60 s until no indentation remained on the material surface. The time at which this occurred was recorded as the initial setting time. The final setting time (elapsed time from the start of mixing until no indentation was observed) was determined using a heavier Gilmore-type needle (diameter: 1.0 mm ± 0.1 mm, weight: 456.5 g ± 5 g) every 5 min until no indentation remained on the material surface.

Solubility

A total of 280 specimens (70 per time point: 1, 7, 14, and 28 days) were fabricated to be used with a well-known method.[27] Each group included 12 replicates of the HCSCs and control. Molds with a diameter of 7.75 mm ± 0.1 mm and height of 1.5 mm ± 0.1 mm were utilized for specimen fabrication.

The molds were placed on a glass plate and filled with the materials. Following 1 h incubation period at 37°C and 95% relative humidity, the specimens were carefully demolded, gently surface-dried using absorbent paper, and transferred to a drying chamber maintained at 37°C for 24 h. Triplicate measurements determined the initial mass of each specimen on an analytical balance (Accuris Dx Series, Benchmark Scientific, NJ USA) with a precision of 0.0001 g. The average of these three measurements was recorded. Specimens were then submerged individually in 7.5 mL of deionized water (pH = 7.4) for their designated immersion time (1, 7, 14, or 28 days). Following immersion, specimens were retrieved, surface-dried with absorbent paper, and placed in a drying chamber at 37°C for 24 h. The final mass of each specimen was determined using the same triplicate weighing procedure employed for initial mass measurement. Each specimen's weight loss (initial mass minus final mass) was expressed as a percentage of the original mass (solubility).

pH in soaking media

Following the completion of the solubility test at each designated time point (1, 7, 14, and 28 days) and after carefully removing the specimens from their respective tubes, eight randomly selected tubes of each group were subjected to pH measurement. The pH was determined using a pre-calibrated digital pH meter (Digimed, Digicrom Analitica, Campo Grande, Brazil) at a constant temperature of 25°C.

Calcium/phosphate nucleation (bioactivity)

Forty-eight specimens (diameter: 8.0 mm ± 0.1 mm; height: 1.6 mm ± 0.1 mm) were fabricated, two per group for four immersion time points: 1, 7, 14, and 28 days. Following preparation, the specimens were vertically immersed in individual containers holding 5 mL of Dulbecco's Phosphate-Buffered Saline (DPBS) solution and hermetically sealed. The containers were maintained at 37°C for the designated immersion periods. A control group of all materials was exposed to double distilled water (DDW) instead of DPBS solution. The

DPBS solution was replaced weekly. After immersion, each specimen was vacuum-desiccated. Subsequently, one specimen from each pair was analyzed using the SEM equipped with EDX. EDX data was used to quantify the surface ratio of calcium/phosphate precipitate. The surface of the remaining specimens from each pair soaked in DPBS solution was scraped for XRD phase analysis. Phase identification was performed using search-match software and the ICDD database (Newtown Square, PA, USA).

Statistical analysis

The normality of data was assessed using the Kolmogorov-Smirnov test. One-way analysis of variance (ANOVA) was performed, followed by a post hoc Tukey's multiple comparison test or the Kruskal–Wallis test, followed by Dunn's test when appropriate. All statistical analyses were conducted using GraphPad Prism version 3.0 (GraphPad Software, San Diego, CA, USA). Statistical significance was set at $p < 0.05$.

Results

The production cost of the HCSC prototypes was significantly lower (USD 3–6 per 10 g of powder, depending on the prototype) than that of commercially available MTA (USD 75 per g of MTA Angelus powder). The scanning electron micrographs of the powder and set forms are displayed in Figure 1. All the powders consisted mainly of small and irregular particles, with some larger ones interspersed. MTA Angelus showed a more noticeable presence of radiopacifier particles. In contrast, fewer radiopacifier particles were observed in the prototypes with 17.5 wt. % replacement (w175 and z175), and more in those with 20 wt. % replacement (w175z25 and w10z10). This difference is evident in the micrographs due to the heavier atomic mass of the radiopacifier particles, making them appear bright and electron-dense. At higher magnification, the smaller particles were seen to cluster around the larger ones. Regarding the set forms, all of them exhibited a smooth surface morphology, with large particles joined by clusters of smaller ones being more evident. All shared similar characteristics with MTA Angelus; however, in the case of the last, the presence of the radiopacifier was even more evident.

The elemental analysis (Figure 1 and Table 2) of the powder and set forms indicated that all were primarily composed of calcium, silicon, and aluminum. Additionally, a significant percentage of the corresponding radiopacifier (zirconium or tungsten) was observed, in line with expectations for each case. MTA Angelus presented the lower aluminum content, followed by the w175, which, in turn, presented the highest calcium content. In addition, XRD data of all the HCSC powders exhibited di- and tri-calcium silicate peaks and tricalcium aluminate ($Ca_3Al_2O_6$). MTA Angelus, w175, w10z10, and w175z25 showed calcium tungstate ($CaWO_4$), while z175, w10z10, and w175z25 showed zirconium oxide (ZrO_2). Only the prototypes showed the presence of calcite ($CaCO_3$) (Figure 2).

Regarding the radiopacity, all materials exhibited radiopacity exceeding 3 mm of aluminum (Table 3). Among the HCSCs, MTA Angelus displayed the greatest radiopacity, significantly ($p < 0.05$) different from all prototypes. Conversely, the w175 and z175 prototypes showed the lowest, with no significant ($p > 0.05$) difference between them, while the w175z25 and w10z10 prototypes were also similar ($p > 0.05$).

Most prototypes exhibited significantly ($p < 0.05$) shorter initial and final setting times than MTA Angelus. The w175 and z175 prototypes had the shortest initial and final setting times, followed by the w175z25 prototype, while the w10z10 prototype exhibited setting times similar ($p > 0.05$) to those of MTA Angelus (Table 3).

The solubility presented by the MTA Angelus, the w175, and the z175 prototypes adhered closely to the ISO standard recommendation of 3% after 1 day of immersion. However, a significant ($p < 0.05$) solubility increase was observed over time in all cases. Notably, the prototypes with the highest radiopacifier content (w175z25 and w10z10) exhibited the greatest solubility, which differed statistically ($p < 0.05$) from that of MTA Angelus. The w175 prototype exhibited the lowest solubility in all experimental periods (Figure 3).

Regarding pH in soaking media, all the HCSCs promoted an alkaline pH. MTA Angelus consistently displayed the highest ($p < 0.05$) pH throughout all observation periods, while the w10z10 prototype generally showed the lowest ($p < 0.05$). The pH of all HCSCs significantly ($p < 0.05$) decreased over time, with the lowest pH values observed at 28 days (Figure 3).

During the bioactivity evaluation, SEM analysis of specimens soaked in DDW revealed that the HCSCs containing only calcium tungstate (MTA Angelus and w175) exhibit an irregular surface with round formations. In contrast, the prototypes containing zirconium oxide alone or in combination with calcium tungstate have smooth surfaces without round formations. In all cases, from the first to 28 days of soaking in DPBS solution, a multi-layered irregular precipitate composed primarily of aggregated spherulites (spherical crystals) was observed. These agglomerates and precipitates altered the surface topography of all the HCSCs, increasing their irregularities and unevenness. The thickness of the precipitate layer on all materials appears to increase progressively with soaking time. This suggests the formation of calcium/phosphate precipitates on the surface (Figure 4). EDX analysis revealed calcium, silicon, aluminum, and phosphorus peaks in all the HCSCs. As expected, tungsten peaks were present in the MTA Angelus, w175, w175z25, and w10z10 prototypes. At the same time, zirconium was only observed in the z175, w175z25, and w10z10 prototypes (Figure 4). Specimens without exposition to DPBS solution showed

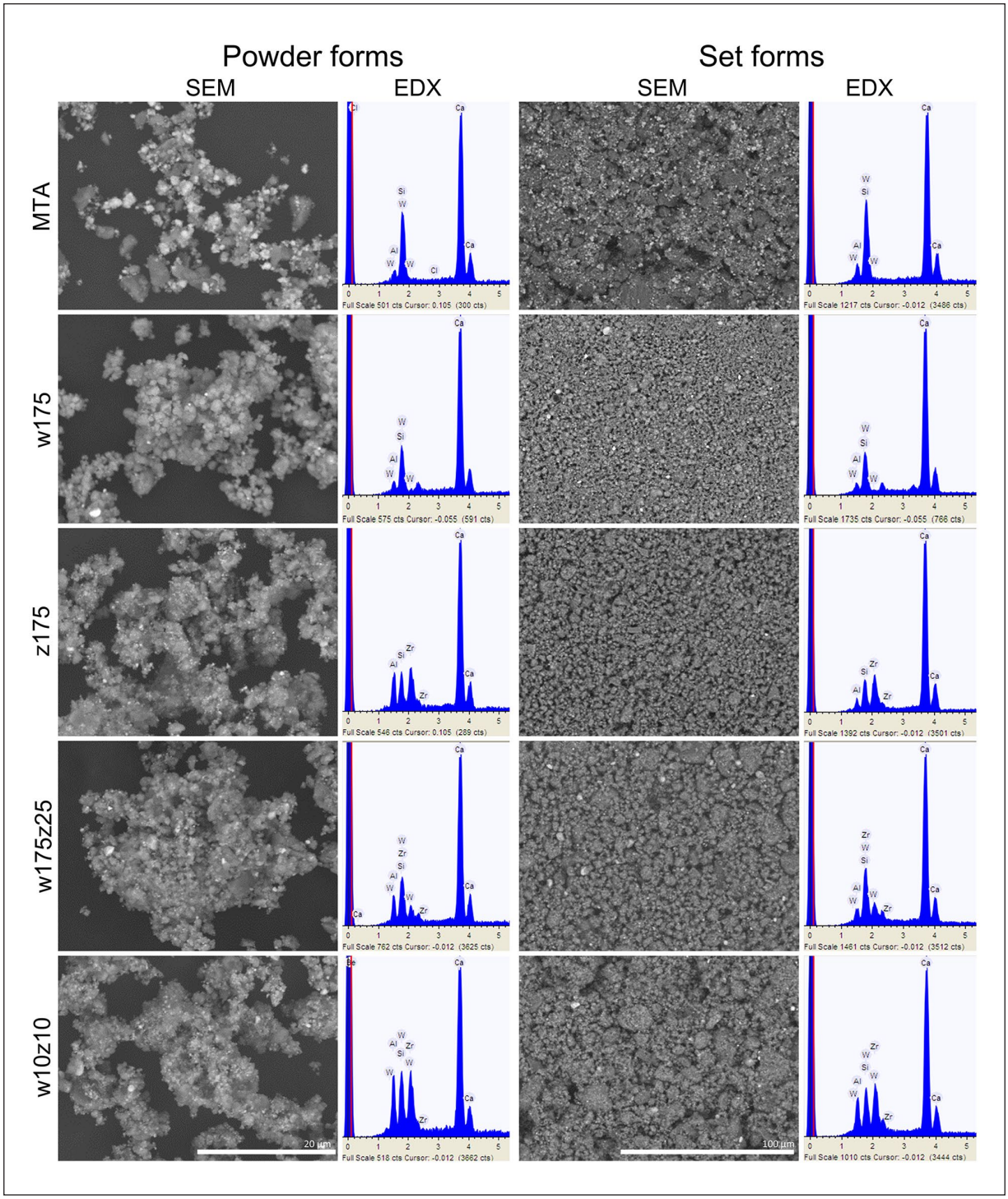

Figure 1. Scanning electron micrographs and corresponding energy-dispersive X-ray spectroscopy analysis (in keV) of MTA Angelus and the four HCSC prototypes in their powder (×4000 magnification) and set (×1000 magnification) forms.

minimum phosphorus content. However, the phosphorus peaks increased in the DPBS-exposed ones at different soaking times, resulting in their highest calcium/phosphate ratio after 1 day for the MTA Angelus, w175, and z175 prototypes. Conversely, the w175z25 and w10z10 prototypes exhibited their higher calcium/phosphate ratios after 7 and 28 days, respectively (Table 4). Notably, silicon became almost undetectable in all materials after soaking. During XRD analysis of the surface precipitates peaks corresponding to hydroxylapatite ($Ca_5(PO_4)_3(OH)$) and halite (NaCl) were clearly detected in all prototypes and MTA Angelus (Figure 5).

Table 2. Elemental composition (wt %), by EDX of the HCSCs in powder and set forms.

Elements	MTA ($n=3$)	w175 ($n=3$)	z175 ($n=3$)	w175z25 ($n=3$)	w10z10 ($n=3$)
	Mean ± standard deviation				
Aluminum					
Powder	2.55 ± 0.64	4.30 ± 2.10	7.80 ± 0.14	5.65 ± 0.35	11.05 ± 4.31
Set	2.65 ± 0.35	3.05 ± 1.20	2.35 ± 0.07	2.65 ± 0.35	6.10 ± 0.28
Silicon					
Powder	6.05 ± 0.78	6.43 ± 0.15	6.95 ± 0.92	4.75 ± 0.35	4.45 ± 0.64
Set	5.90 ± 0.28	5.40 ± 0.71	6.20 ± 0.14	4.95 ± 0.21	4.35 ± 0.49
Calcium					
Powder	69.45 ± 3.04	73.56 ± 1.35	66.25 ± 0.21	68.20 ± 1.13	55.45 ± 7.57
Set	64.60 ± 1.84	78.30 ± 0.0	73.20 ± 0.71	66.45 ± 0.49	61.90 ± 4.67
Zirconium					
Powder	0	0	19.00 ± 0.42	7.55 ± 0.07	19.25 ± 2.23
Set	0	0	18.20 ± 0.57	9.65 ± 1.20	18.80 ± 2.12
Tungsten					
Powder	21.90 ± 2.83	15.70 ± 1.21	0	13.90 ± 0.99	9.70 ± 0.28
Set	26.90 ± 1.84	13.20 ± 0.42	0	9.65 ± 1.20	8.80 ± 2.69

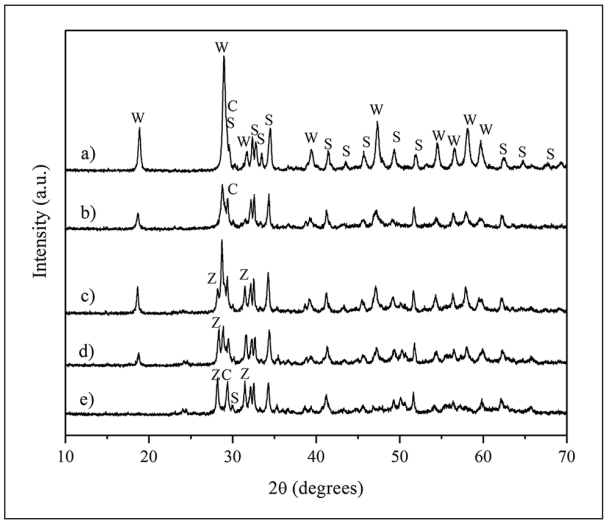

Figure 2. X-ray diffraction patterns of the HCSCs. (a) MTA Angelus, (b) w175, (c) w175z25, (d) w10z10, (e) z175.
W: scheelite ($CaWO_4$); C: calcite ($CaCO_3$); S: calcium silicates (Ca_3SiO_5, Ca_2SiO_4) and calcium aluminate ($Ca_3Al_2O_6$); Z: baddeleyite (ZrO_2).

Discussion

VPT offers a promising approach to reducing tooth loss in populations with limited access to root canal treatment, particularly those relying on public healthcare.[7] However, a significant obstacle remains: the high cost of commercially available HCSCs impedes their widespread use in public dental services. To address this limitation, we have leveraged existing knowledge of HCSCs to design and produce low-cost prototypes. These HCSC prototypes prioritize optimal physical, mechanical, and biological properties through affordable and readily available high-purity laboratory-grade ingredients within a university setting. All our prototypes boast a mean production cost that is at least 150 times lower than the actual cost of commercial MTA (MTA Angelus).

Most of the results from this investigation demonstrate excellent physical properties in all prototypes, comparable to those of MTA Angelus, a well-known and positioned commercial material. Some of them performed even better than MTA Angelus, while others met the minimum requirements for VPT applications.

All the prototype powders generally consisted of slightly finer particles than the MTA Angelus powder but with the same irregular appearance when examined using SEM. This difference in particle size was more evident in the set forms, where larger particles were observed embedded within the MTA Angelus matrix but not in the z175 nor the w175 prototypes. Their chemical composition was very similar, with only the expected variations attributable to their formulation. To the best of our knowledge, this is the first investigation where two radiopacifiers have been simultaneously incorporated into the individual preparation of an HCSC; both are widely used and have documented efficacy.[28] They allow calcium release and maintain an alkaline pH, while neither induces tooth discoloration.[29,30] They exhibit minimal biological reactivity, and their combination has been used in a popular endodontic sealer known for its excellent radiopacity, AH Plus.[31] Achieving sufficient radiopacity is essential for clinical practice, as it enables clear visualization of the material within the tooth structure during radiographic examinations. This ensures proper placement and verifies the material's placement within the intended area. However, it is well documented that these additives can interact with surrounding tissues, potentially leading to adverse biological effects. The potential impact of these specific radiopacifiers on these

Table 3. Radiopacity (mm of aluminum) and setting time (initial and final in minutes) of the HCSCs and control.

Physical property	MTA	w175	z175	w175z25	w10z10	*p*-Value	IRM
	Mean ± standard deviation						
Radiopacity	(*n* = 8)	(*n* = 8)	(*n* = 8)	(*n* = 8)	(*n* = 8)		(n=8)
	5.60 ± 0.13	3.91 ± 0.12	3.99 ± 0.11	4.87 ± 0.07	5.09 ± 0.20	<0.0001	5.70 ± 0.29
Setting time	(*n* = 5)	(*n* = 5)	(*n* = 5)	(*n* = 5)	(*n* = 5)		(n=5)
Initial	16.6 ± 0.54	9.4 ± 0.54	9.0 ± 0.00	10.4 ± 0.54	16.6 ± 0.54	<0.0001	1.8 ± 0.44
Final	82.0 ± 2.73	61.0 ± 2.23	63.0 ± 2.73	69.0 ± 2.23	72.0 ± 2.73	<0.0001	6.0 ± 2.23

ANOVA was applied in all comparisons. The Tukey-Kramer multiple comparison tests indicated significant differences in all comparisons except when comparing radiopacity: z175 versus w175 and w175z25 versus w10z10. Initial setting time: MTA versus w10z10 and w175 versus z175. Final setting time: w175 versus z175 and w175z25 versus w10z10.

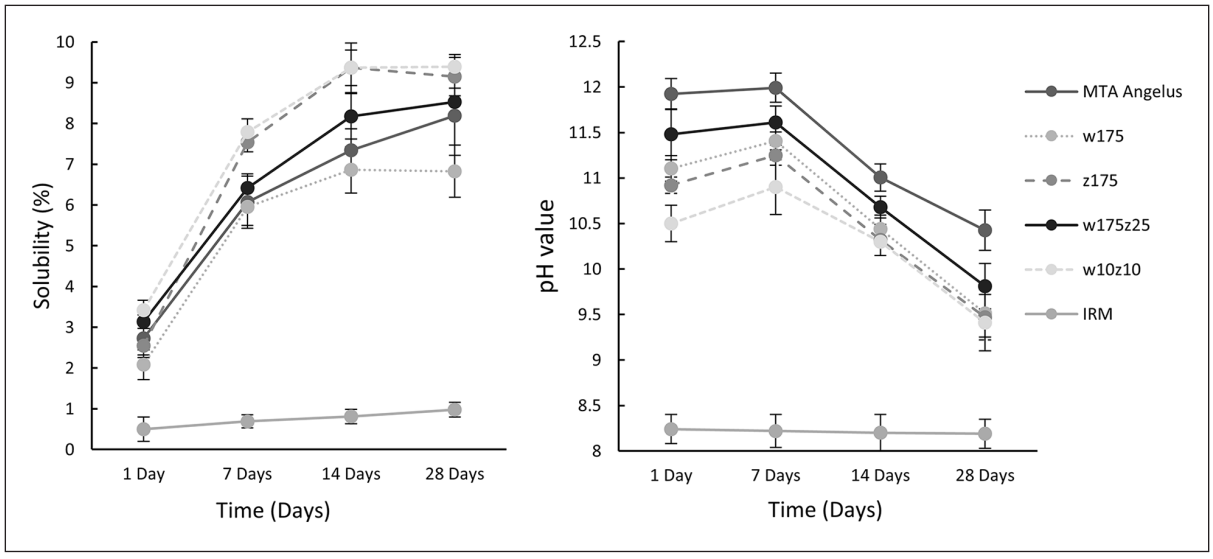

Figure 3. Solubility (%) and pH values (means and standard deviations) of the tested HCSC and IRM. The Kruskal–Wallis test was used to compare solubility values, while ANOVA was used to compare pH values. All differences were statistically significant ($p < 0.0001$; Supplemental Table 1). Multiple comparisons are shown in Supplemental Tables 2 and 3.

prototypes is currently under investigation in ongoing research. During the design of the prototypes, a critical balance was sought between achieving radiopacity and minimizing the amount of radiopacifying agents incorporated into the formula. All prototypes achieved a radiopacity exceeding the ISO 4049 standard (>3 mm aluminum equivalent). Among the developed prototypes, w10z10 and w175z25 demonstrated the highest radiopacity, while those with a lower radiopacifier content (17.5 wt. %) exhibited the minimum values. As expected, MTA Angelus, which also contains calcium tungstate as a radiopacifier, displayed the highest radiopacity. The specific amount used in MTA Angelus remains undisclosed by the manufacturer. However, our EDX analysis showed a higher proportion of tungsten than the prototypes, which explains the observed difference in radiopacity. Interestingly, these radiopacity findings appear to be inversely correlated with the results obtained in the setting time tests; it is well known that the amount of additives influences the setting time.

One of the most discussed properties of HCSCs is their setting time, mainly since the first commercially available, the ProRoot MTA (Dentsply Tulsa Dental, Tulsa, OK, USA) exhibited an extended setting time (up to 2.5 h) while for the MTA Angelus, it has been reported in 80 min.[32] A lengthy setting time can hinder clinical performance by making the material susceptible to washout from the prepared cavity due to biological fluids or irrigation solutions, posing challenges for the dentist. To address this limitation, extensive research has been conducted to explore strategies for reducing the setting time of HCSCs.[33–41] These strategies include setting accelerators and optimizing particle size and the powder-to-liquid ratio.[42] These principles guided the design of our prototypes. We achieved a fine particle size and established the optimal powder-to-liquid ratio, ensuring a consistency suitable for clinical applications. Additionally, we reduced the radiopacifier content to a maximum of 20 wt. %, compared to the generally reported 25 wt. % in commercial

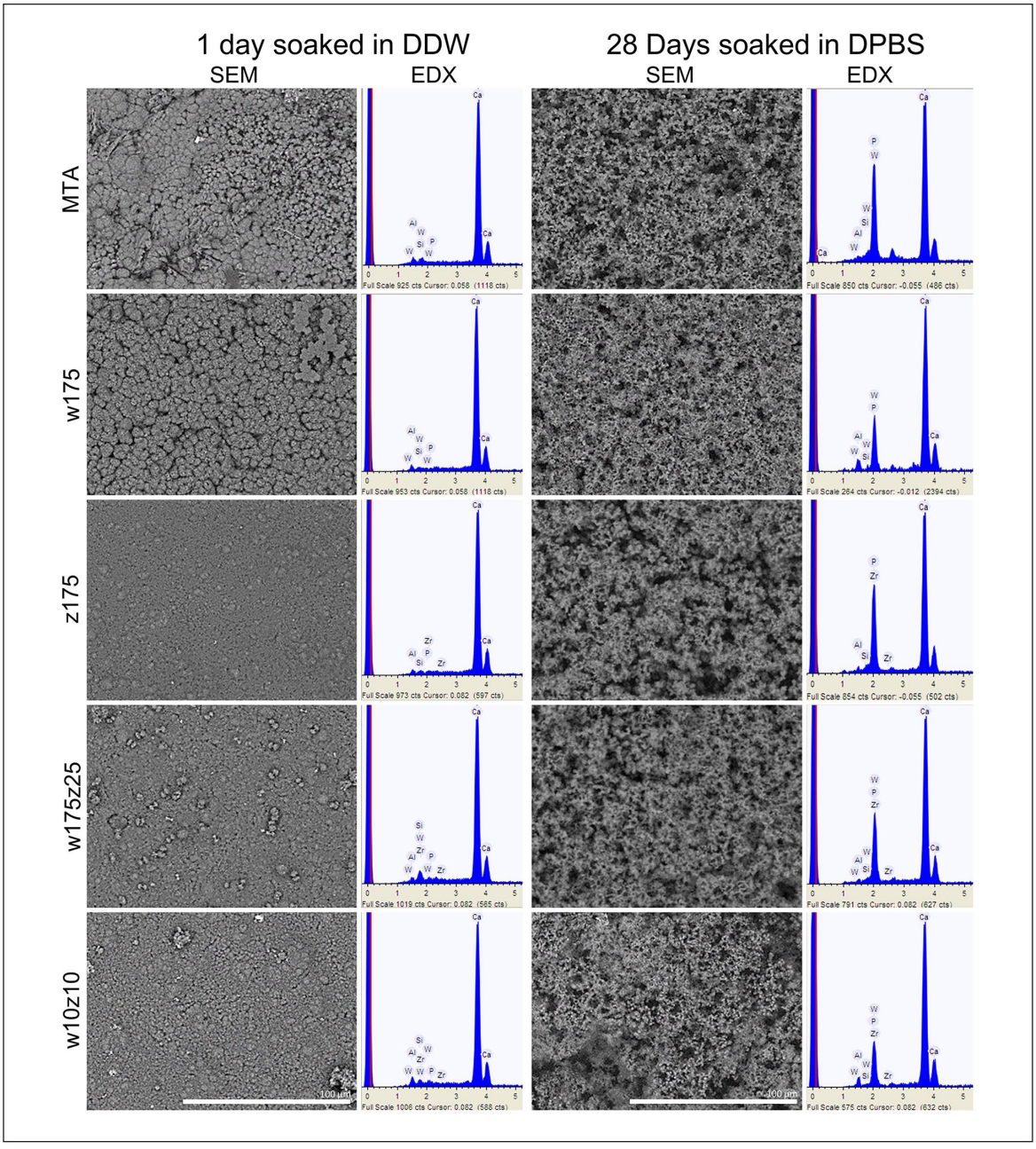

Figure 4. Representative scanning electron micrographs and corresponding energy-dispersive X-ray spectroscopy analysis (in keV) of MTA Angelus and the four HCSC prototypes. Representative analysis of specimens soaked in double-distilled water (DDW) for one day or in Dulbecco's Phosphate-Buffered Saline (DPBS) solution for 28 days (×1000 magnification).

Table 4. Calcium/phosphate ratio of the HCSCs after soaking in DPBS solution.

Time point	MTA ($n=3$)	w175 ($n=3$)	z175 ($n=3$)	w175z25 ($n=3$)	w10z10 ($n=3$)
	Ca/P ratio				
1 day	5.49	5.54	4.49	3.94	4.72
7 days	4.05	4.95	4.31	4.68	5.44
14 days	3.57	3.55	4.29	4.56	6.71
28 days	2.88	2.55	3.17	3.61	8.26

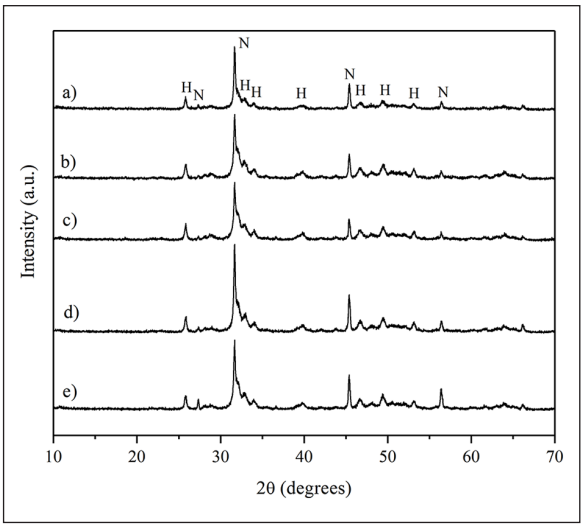

Figure 5. X-ray diffraction patterns of the hydroxylapatite and halite produced by the prototypes (a) MTA Angelus, (b) w175, (c) w175z25, (d) w10z10, and (e) z175.
H: hydroxylapatite ($Ca_5(PO_4)_3(OH)$); N: halite (NaCl).

MTA. This reduction resulted in shorter setting times with minimal incorporation (17.5 wt. %). This is in agreement with previous reports[43–45] that suggest that a minimal quantity of radiopacifier could be crucial for optimal setting time because the larger amounts of cement in these mixtures allow better hydration but also because diminishing the particle size increases the amount of its surface area that come into contact with water.[46] All this also contributed to minimizing their solubility.

Solubility of HCSCs is crucial for achieving a long-lasting seal and preventing leakage. The ISO 6876/2002 standard mandates solubility evaluation after 24 h, although extended evaluation periods are commonly used.[47,48] In this study, all the materials exhibited solubility values below the recommended 3% limit established by the ISO standard at the 24-h mark. MTA Angelus showed a solubility in agreement with another study,[43] while single radiopacifier prototypes (w175 and z175) exhibited the lowest solubility at 24 h, with no significant differences compared to MTA Angelus. Conversely, prototypes with two radiopacifiers (w175z25 and w10z10) exhibited the highest solubility values. This suggests a potential correlation, where a lower cement-to-radiopacifier ratio might have hindered the hydration process. It is well known that the solubility of the HCSCs is influenced by the formation of soluble calcium salts and calcium hydroxide during the hydration and setting reactions of the material[14] but also by the water-to-powder ratio. Increasing the water content increases solubility.[49,50] Adjustments to this ratio can also modify other properties, such as calcium ion release and flow characteristics.[51] Mixing these prototypes was prioritized using an optimal water-to-powder ratio to achieve the desired balance between these properties. Still, these were the best characteristics that could be obtained for them.

Regarding pH, all HCSCs induced rapid medium alkalinization, peaking between 7 and 14 days. Subsequently, a gradual decrease in pH was observed at 28 days, aligning with previous reports[32,37] of decreased alkalinizing activity over time. The initial pH rise is attributed to the combined effects of calcium hydroxide formation and calcium ion release from the dissolving calcium silicate particles.[32,52] While MTA Angelus exhibited the highest pH values, consistent with previous findings,[32,37] all the prototypes presented an alkaline pH, with the lowest value only 1 unit below MTA Angelus. It has been reported that ion release from HCSCs is influenced by several factors, including the size, density, and distribution of mineral particles (calcium hydroxide or unhydrated cement particles). Additionally, the hydrated cement matrix's network structure, particularly the calcium silicate hydrate phase, significantly impacts water sorption, solubility, and permeability.[53] These findings suggest that all prototypes are suitable for acidic environments due to their pH-mediated antimicrobial properties, a well-established concept.[54,55] Furthermore, the elevated pH may also promote tissue healing processes.[32,56] However, the formation of calcium/phosphate precipitate when they come into contact with phosphate-containing physiological fluids, known as bioactivity,[57,58] plays a positive role in cell attachment and differentiation but also within tissue mineralization.[14,59,60] Also, the calcium/phosphate precipitate formation is known to contribute to the occlusion of dentinal tubules[61] and the sealing of the material–dentine interface,[62,63] both essential in a material that will be used in VPT. The calcium/phosphate precipitate forms via the dissolution of the calcium hydroxide that forms during the initial hydration reaction, which causes increases in pH and the calcium ion concentration and enhances the supersaturation of the phosphate-containing fluid, promoting precipitation.[64]

All the HCSCs tested in this investigation demonstrated the ability to produce calcium/phosphate precipitates, which displayed a spherical appearance with acicular microprojections and contained calcium and phosphate as their main elements. Silicon was almost completely absent on the aged specimens' surface, while the phosphate component prevailed. Nevertheless, the findings are consistent with the observation that precipitates are uniformly formed on all HCSCs after 7 days of DPBS immersion.

The early immersion periods suggest that the precipitates were less "mature" than those in more extensive periods. However, XRD peaks corresponding to hydroxylapatite were detected in all time point precipitates. In most prototypes, the calcium/phosphate ratios were higher than that obtained on the MTA Angelus. In contrast, the ratio obtained by this at 28 days was consistent with a previous report of 2.05.[37] The w10z10 prototype produced the precipitates with lower calcium/phosphate ratios than the other HCSCs.

While the results of this study suggest the potential application of all tested prototypes in VPT, their physical

properties represent only one aspect of the requirements for a dental cement. Further research is ongoing to fully evaluate the prototypes' mechanical and biological properties, while preliminary results seem promising.

Conclusion

All prototypes exhibited physical properties comparable to or exceeding those of MTA Angelus, including an alkalizing pH, appropriate solubility, radiopacity, and faster initial and final setting times. Additionally, they demonstrated the ability to form calcium/phosphate precipitates. These promising findings suggest their potential application in VPT. However, further investigation is necessary to assess their mechanical and biological properties for definitive clinical translation.

Acknowledgements

The authors want to thank to "Proyecto Ciencia de Frontera" by the Mexican National Council for Humanities, Science and Technology (CONAHCYT) and the Secretariat of Research, Innovation, and Postgraduate Studies of the Universidad Autónoma de Querétaro.

Author contributions

Conceptualization: MV-G, RAD-P; methodology: MV-G, RAD-P, LFE-C, RD-P, RGSL-T; formal analysis: RAD-P, AEH-M, LFE-C; investigation: MV-G, RAD-P, AEH-M, LFE-C, RD-P, RGS-LT; writing – original draft preparation: MV-G, RAD-P; writing – review and editing: MV-G, RAD-P, AEH-M, LFE-C, RD-P, RGS-LT; supervision: AEH-M, RGS-LT; project administration, RAD-P, RDP; funding acquisition: RAD-P, MV-G, AEH-M. All authors have read and agreed to the published version of the manuscript.

Data availability statement

The data used to support the findings of this study are available from the corresponding author upon reasonable request.

Declaration of conflicting interests

The author(s) declared no potential conflicts of interest with respect to the research, authorship, and/or publication of this article.

Funding

The author(s) disclosed receipt of the following financial support for the research, authorship, and/or publication of this article: This research was funded by the Mexican National Council for Humanities, Science and Technology (CONAHCYT) through the program "Frontiers of Science 2023 – Ciencia de Frontera 2023," Grant Number "CF-2023-G-29."

ORCID iDs

Rubén Abraham Domínguez-Pérez https://orcid.org/0000-0001-8979-8394
León Francisco Espinosa-Cristóbal https://orcid.org/0000-0002-9295-6928

Supplemental material

Supplemental material for this article is available online.

References

1. Lee SJ, Monsef M and Torabinejad M. Sealing ability of a mineral trioxide aggregate for repair of lateral root perforations. *J Endod* 1993; 19: 541–544.
2. Gandolfi MG, Taddei P, Tinti A, et al. Apatite-forming ability (bioactivity) of ProRoot MTA. *Int Endod J* 2010; 43: 917–929.
3. Çalışkan MK, Tekin U, Kaval ME, et al. The outcome of apical microsurgery using MTA as the root-end filling material: 2-to 6-year follow-up study. *Int Endod J* 2016; 49: 245–254.
4. Krupp C, Bargholz C, Brüsehaber M, et al. Treatment outcome after repair of root perforations with mineral trioxide aggregate: a retrospective evaluation of 90 teeth. *J Endod* 2013; 39: 1364–1368.
5. Bonte E, Beslot A, Boukpessi T, et al. MTA versus Ca (OH) 2 in apexification of non-vital immature permanent teeth: a randomized clinical trial comparison. *Clin Oral Investig* 2015; 19: 1381–1388.
6. Li Z, Cao L, Fan M, et al. Direct pulp capping with calcium hydroxide or mineral trioxide aggregate: a meta-analysis. *J Endod* 2015; 41: 1412–1417.
7. Sánchez-Lara y, Tajonar RG, Vergara-Tinoco JV, Dammaschke T, et al. A pilot feasibility study to establish full pulpotomy in mature permanent teeth with symptomatic irreversible pulpitis as a routine treatment in mexican public healthcare services. *Healthcare* 2022; 10: 2350.
8. Dammaschke T, Gerth HUV, Züchner H, et al. Chemical and physical surface and bulk material characterization of white ProRoot MTA and two Portland cements. *Dent Mater* 2005; 21: 731–738.
9. Vallés M, Mercadé M, Duran-Sindreu F, et al. Color stability of white mineral trioxide aggregate. *Clin Oral Investig* 2013; 17: 1155–1159.
10. Purra AR, Ahangar FA, Chadgal S, et al. Mineral trioxide aggregate apexification: a novel approach. *J Conserv Dent Endod* 2016; 19: 377–380.
11. Viola NV, Tanomaru Filho M and Cerri PS. MTA versus Portland cement: review of literature. *RSBO* 2011; 8: 446–452.
12. Yong D, Choi JJE, Cathro P, et al. Development and analysis of a hydroxyapatite supplemented calcium silicate cement for endodontic treatment. *Materials (Basel)* 2022; 15: 1176.
13. Eskandari F, Razavian A, Hamidi R, et al. An updated review on properties and indications of calcium silicate-based cements in endodontic therapy. *Int J Dent* 2022; 2022: 1–19.
14. Gandolfi MG, Siboni F, Botero T, et al. Calcium silicate and calcium hydroxide materials for pulp capping: biointeractivity, porosity, solubility and bioactivity of current formulations. *J Appl Biomater Funct Mater* 2015; 13: 43–60.
15. Gandolfi MG, Taddei P, Modena E, et al. Biointeractivity-related versus chemi/physisorption-related apatite precursor-forming ability of current root end filling materials. *J Biomed Mater Res Part B Appl Biomater* 2013; 101: 1107–1123.
16. Singh S, Podar R, Dadu S, et al. Solubility of a new calcium silicate-based root-end filling material. *J Conserv Dent Endod* 2015; 18: 149–153.

17. Bortoluzzi EA, Broon NJ, Bramante CM, et al. Sealing ability of MTA and radiopaque Portland cement with or without calcium chloride for root-end filling. *J Endod* 2006; 32: 897–900.
18. Camilleri J and Gandolfi MG. Evaluation of the radiopacity of calcium silicate cements containing different radiopacifiers. *Int Endod J* 2010; 43: 21–30.
19. Gandolfi MG, Iacono F, Agee K, et al. Setting time and expansion in different soaking media of experimental accelerated calcium-silicate cements and ProRoot MTA. *Oral Surg Oral Med Oral Pathol Oral Radiol Endod* 2009; 108: e39–e45.
20. de Souza LC, Yadlapati M, Dorn SO, et al. Analysis of radiopacity, pH and cytotoxicity of a new bioceramic material. *J Appl Oral Sci* 2015; 23: 383–389.
21. Shen YA, Peng B, Yang Y, et al. What do different tests tell about the mechanical and biological properties of bioceramic materials? *Endod Top* 2015; 32: 47–85.
22. Mitragotri S and Lahann J. Physical approaches to biomaterial design. *Nat Mater* 2009; 8: 15–23.
23. Khurshid Z, Alqurashi H and Ashi H. Advancing environmental sustainability in dentistry and oral health. *Eur J Gen Dent* 2024; 13: 264–268.
24. Angelus Indústria de Produtos Odontológicos S/A. *Angelus MTA (package insert)*. Londrina, PR, Brasil: Angelus Indústria de Produtos Odontológicos S/A, 2024.
25. Dentsply Caulk. *Intermediate Restorative Material (package insert)*. Milford, DE: Dentsply Caulk, 2024.
26. ASTM C. 266-08. *Standard test method for time of setting of hydraulic-cement paste by gilmore needles*. West Conshohocken, PA: ASTM Int.
27. Torres FFE, Guerreiro-Tanomaru JM, Bosso-Martelo R, et al. Solubility, porosity and fluid uptake of calcium silicate-based cements. *J Appl Oral Sci* 2018; 26: 1–8.
28. Duarte MAH, de Oliveira GDE, Vivan RR, et al. Radiopacity of Portland cement associated with different radiopacifying agents. *J Endod* 2009; 35: 737–740.
29. Kang SH, Shin YS, Lee HS, et al. Color changes of teeth after treatment with various mineral trioxide aggregate–based materials: an ex vivo study. *J Endod* 2015; 41: 737–741.
30. Marciano MA, Costa RM, Camilleri J, et al. Assessment of color stability of white mineral trioxide aggregate angelus and bismuth oxide in contact with tooth structure. *J Endod* 2014; 40: 1235–1240.
31. Tanomaru-Filho M, Jorge ÉG, Tanomaru JMG, et al. Radiopacity evaluation of new root canal filling materials by digitalization of images. *J Endod* 2007; 33: 249–251.
32. Prati C and Gandolfi MG. Calcium silicate bioactive cements: biological perspectives and clinical applications. *Dent Mater* 2015; 31: 351–370.
33. Jiménez-Sánchez MC, Segura-Egea JJ and Díaz-Cuenca A. Higher hydration performance and bioactive response of the new endodontic bioactive cement MTA HP repair compared with ProRoot MTA white and NeoMTA plus. *J Biomed Mater Res* 2019; 107: 2109–2120.
34. Asgary S, Shahabi S, Jafarzadeh T, et al. The properties of a new endodontic material. *J Endod* 2008; 34: 990–993.
35. Dawood AE, Parashos P, Wong RHK, et al. Calcium silicate-based cements: composition, properties, and clinical applications. *J Investig Clin Dent* 2017; 8: 1–15.
36. Kim M, Yang W, Kim H, et al. Comparison of the biological properties of ProRoot MTA, OrthoMTA, and Endocem MTA cements. *J Endod* 2014; 40: 1649–1653.
37. Guimarães BM, Prati C, Duarte MAH, et al. Physicochemical properties of calcium silicate-based formulations MTA repair HP and MTA Vitalcem. *J Appl Oral Sci* 2018; 26: 1–8.
38. Santos AD, Araújo EB, Yukimitu K, et al. Setting time and thermal expansion of two endodontic cements. *Oral Surg Oral Med Oral Pathol Oral Radiol Endod* 2008; 106: 77–79.
39. Dawood AE, Manton DJ, Parashos P, et al. The physical properties and ion release of CPP-ACP-modified calcium silicate-based cements. *Aust Dent J* 2015; 60: 434–444.
40. Zamparini F, Siboni F, Prati C, et al. Properties of calcium silicate-monobasic calcium phosphate materials for endodontics containing tantalum pentoxide and zirconium oxide. *Clin Oral Investig* 2019; 23: 445–457.
41. Jiménez-Sánchez MC, Segura-Egea JJ and Díaz-Cuenca A. A microstructure insight of MTA repair HP of rapid setting capacity and bioactive response. *Materials (Basel)* 2020; 13: 1–12.
42. Camilleri J, Cutajar A and Mallia B. Hydration characteristics of zirconium oxide replaced Portland cement for use as a root-end filling material. *Dent Mater* 2011; 27: 845–854.
43. Duarte MAH, Minotti PG, Rodrigues CT, et al. Effect of different radiopacifying agents on the physicochemical properties of white Portland cement and white mineral trioxide aggregate. *J Endod* 2012; 38: 394–397.
44. Camilleri J. Hydration mechanisms of mineral trioxide aggregate. *Int Endod J* 2007; 40: 462–470.
45. Camilleri J. Evaluation of the physical properties of an endodontic Portland cement incorporating alternative radiopacifiers used as root-end filling material. *Int Endod J* 2010; 43: 231–240.
46. Camilleri J, Formosa L and Damidot D. The setting characteristics of MTA plus in different environmental conditions. *Int Endod J* 2013; 46: 831–840.
47. Bosso-Martelo R, Guerreiro-Tanomaru JM, Viapiana R, et al. Physicochemical properties of calcium silicate cements associated with microparticulate and nanoparticulate radiopacifiers. *Clin Oral Investig* 2016; 20: 83–90.
48. Torres FFE, Bosso-Martelo R, Espir CG, et al. Evaluation of physicochemical properties of root-end filling materials using conventional and Micro-CT tests. *J Appl Oral Sci* 2017; 25: 374–380.
49. Fridland M and Rosado R. MTA solubility: a long term study. *J Endod* 2005; 31: 376–379.
50. Cavenago BC, Pereira TC, Duarte MAH, et al. Influence of powder-to-water ratio on radiopacity, setting time, pH, calcium ion release and a micro-CT volumetric solubility of white mineral trioxide aggregate. *Int Endod J* 2014; 47: 120–126.
51. Camilleri J, Wang C, Kandhari S, et al. Methods for testing solubility of hydraulic calcium silicate cements for root-end filling. *Sci Rep* 2022; 12: 1–13.
52. Gandolfi MG, Van Landuyt K, Taddei P, et al. Environmental scanning electron microscopy connected with energy dispersive X-ray analysis and Raman techniques to study ProRoot mineral trioxide aggregate and calcium silicate cements in wet conditions and in real time. *J Endod* 2010; 36: 851–857.

53. Yamamoto S, Han L, Noiri Y, et al. Evaluation of the Ca ion release, pH and surface apatite formation of a prototype tricalcium silicate cement. *Int Endod J* 2017; 50: e73–e82.
54. Razmi H, Aminsobhani M, Bolhari B, et al. Calcium enriched mixture and mineral trioxide aggregate activities against *Enterococcus faecalis* in presence of dentin. *Iran Endod J* 2013; 8: 191.
55. Al-Hezaimi K, Al-Shalan TA, Naghshbandi J, et al. Antibacterial effect of two mineral trioxide aggregate (MTA) preparations against *Enterococcus faecalis* and Streptococcus sanguis in vitro. *J Endod* 2006; 32: 1053–1056.
56. Costa F, Gomes PS and Fernandes MH. Osteogenic and angiogenic response to calcium silicate–based endodontic sealers. *J Endod* 2016; 42: 113–119.
57. Han L and Okiji T. Bioactivity evaluation of three calcium silicate-based endodontic materials. *Int Endod J* 2013; 46: 808–814.
58. Han L, Kodama S and Okiji T. Evaluation of calcium-releasing and apatite-forming abilities of fast-setting calcium silicate-based endodontic materials. *Int Endod J* 2015; 48: 124–130.
59. Thomson TS, Berry JE, Somerman MJ, et al. Cementoblasts maintain expression of osteocalcin in the presence of mineral trioxide aggregate. *J Endod* 2003; 29: 407–412.
60. Seo M-S, Hwang K-G, Lee J, et al. The effect of mineral trioxide aggregate on odontogenic differentiation in dental pulp stem cells. *J Endod* 2013; 39: 242–248.
61. Yoo JS, Chang S-W, Oh SR, et al. Bacterial entombment by intratubular mineralization following orthograde mineral trioxide aggregate obturation: a scanning electron microscopy study. *Int J Oral Sci* 2014; 6: 227–232.
62. Sarkar NK, Caicedo R, Ritwik P, et al. Physicochemical basis of the biologic properties of mineral trioxide aggregate. *J Endod* 2005; 31: 97–100.
63. Reyes-Carmona JF, Felippe MS and Felippe WT. Biomineralization ability and interaction of mineral trioxide aggregate and white portland cement with dentin in a phosphate-containing fluid. *J Endod* 2009; 35: 731–736.
64. Kokubo T and Takadama H. How useful is SBF in predicting in vivo bone bioactivity? *Biomaterials* 2006; 27: 2907–2915.